Chapter 9
Radiolabeling & Pharmacokinetics of Carvedilol Formulations

9.1 Introduction

9.1.1 Labeling with ^{99m}Tc

More than 80% of radiopharmaceuticals used in nuclear medicine are ^{99m}Tc - labeled compounds due to favorable physical and radiation characteristics of ^{99m}Tc. The 6 h physical half life and the little amount of electron emission permit the administration of millicurie (mCi) amounts of ^{99m}Tc radioactivity without significant radiation dose to the patient. In addition, the monochromatic 140 keV photons are readily collimated to give images of superior spatial resolution. Furthermore, ^{99m}Tc is readily available in a sterile, pyrogen free, and carrier-free state from ^{99}Mo - ^{99m}Tc generators (Saha, 2004).

9.1.2 Chemistry of Technetium

Technetium is a transition metal of silvery gray color belonging to group VIIB (Mn, Tc, Re) and has a half-life of 2.1×10^5 years. The electronic structure of the neutral technetium atom is $1s^2\ 2s^2\ 2p^6\ 3s^2\ 3p^6\ 3d^6\ 3d^{10}\ 4s^2\ 4p^6\ 4d^6\ 5s^1$. Technetium can exist in eight oxidation states, namely 1- to 7+, which result from the loss of a given number of electrons from the 4d and 5s orbitals or gain of an electron to the 4d orbital. The stability of these oxidation states depends on the types of ligands and chemical environment. The 7+ and 4+ states are most stable and exist in oxides, sulfides, halides and pertechnetates.

9.1.3 Reduction of ^{99m}Tc

The chemical form of ^{99m}Tc available from the Moly generator is sodium pertechnetate (^{99m}Tc-$NaTcO_4$). The pertechnetate ion, $^{99m}TcO_4^-$, having the oxidation state 7+ or ^{99m}Tc, resembles the permanganate ion, MnO_4^-, and the perrhenate ion, ReO_4^-. It has a configuration of a pyramidal tetrahedron with Tc^{7+} located at the center and four oxygen atoms at the apex and corners of the pyramid. Chemically $^{99m}TcO_4^-$ is a rather non reactive species and does not label any compound by direct addition. In ^{99m}Tc – labeling of many compounds, prior reduction of ^{99m}Tc from the 7+ state to a lower oxidation state is required. Various reducing agents that have been used are stannous chloride ($SnCl_2.2H_2O$), stannous citrate, stannous tartrate, concentrated HCl,

sodium borohydride ($NaBH_4$), dithionite and ferrous sulphate. Among these, stannous chloride is the most common used reducing agent in most preparations of ^{99m}Tc – labeled compounds.

The chemical reactions that occur in the reduction of technetium by stannous chloride in acidic medium can be stated as follows:

$$3\ Sn^{2+} \longleftrightarrow 3\ Sn^{4+} + 6e^- \quad \text{..... 9.1}$$

$$2\ ^{99m}TcO_4^- + 16\ H^+ + 6e^- \longleftrightarrow 2\ ^{99m}Tc^{4+} + 8\ H_2O \quad \text{..... 9.2}$$

Adding the above two equations, one has

$$2\ ^{99m}TcO_4^- + 16\ H^+ + 3\ Sn^{2+} \longleftrightarrow 2\ ^{99m}Tc^{4+} + 3\ Sn^{4+} + 8\ H_2O \quad \text{..... 9.3}$$

Equation 9.2 indicates that $^{99m}Tc^{7+}$has been reduced to $^{99m}Tc^{4+}$. Other states such as $^{99m}Tc^{3+}$ and $^{99m}Tc^{5+}$ may be formed under different physicochemical conditions. It may also be possible for a mixture of these species to be present in a given preparation. Experiments with millimolar quantities of ^{99m}Tc have shown that Sn^{2+} reduces ^{99}Tc to the 5+ state and then slowly to the 4+ state in citrate buffer at pH 7. Technetium-99 is reduced to the 4+ state by Sn^{2+} in concentrated HCl.

The amount of ^{99m}Tc atoms in the ^{99m}Tc-eluate is very small ($\approx 10^{-9}$ M), and therefore only a minimal amount of Sn^{2+} is required for reduction of such a small quantity of ^{99m}Tc; however enough Sn^{2+} is added to ensure complete reduction. The ratio of Sn^{2+} ions to ^{99m}Tc atoms may be as large as 10^6. The reduced ^{99m}Tc species are chemically reactive and combine with wide variety of compounds bearing chemical groups like – COOH, -OH, $-NH_2$, and –SH (Saha, 2004).

9.1.4 Gamma Scintigraphy

Gamma scintigraphy provides a noninvasive method to 'see' the *in vivo* fate of a pharmaceutical dosage form. The power of the technique is realized fully by correlating deposition and transit of the delivery system with resulting systemic drug levels. Since their inception 25 years ago, these methods have evolved into the preferred technology for evaluation of the *in vivo* behavior of drug delivery systems.

Gamma scintigraphy is a technique by which the transit of a dosage form through its intended site of delivery can be noninvasively imaged *in vivo* via the judicious introduction of an appropriate short-lived, gamma-emitting radioisotope. The observed transit of the dosage form is then correlated with the rate and extent of drug absorption using human subjects or an appropriate animal model. Gamma scintigraphy has proven to be of great value in assisting product development as well as in the testing of marketed products. In a typical scintigraphic procedure, radiated photons from the labeled dosage form or an anatomical site pass through a collimator and strike the sodium-iodide crystal of a gamma camera. The resultant flash of light is subsequently detected by photomultiplier tubes. The analog signal is then digitized and this permits quantitative image processing (Digenis et al., 1998).

9.2 MATERIALS AND METHODS

9.2.1 Materials

- Stannous chloride dihydrate ($SnCl_2.2H_2O$) were purchased from Sigma Chemical Company, St. Louis, MO.
- Sodium pertechnetate, separated from molybdenum-99 (99m) was provided by Regional Center for Radiopharmaceutical Division (Northern Region), Board of Radiation and Isotope Technology, New Delhi, India.
- Instant thin layer chromatography silica gel impregnated fiber sheets (ITLC - SG) were purchased from Gelman Sciences Inc., Ann Arbor, MI.
- MIAT® nasal monodose insufflator device was gift sample from MIAT S.p.A. Milan, Italy.
- Hard gelatin capsules No. 3 were received as the gift sample from Associated Capsules Pvt. Ltd. (A member of ACG Worldwide), Mumbai, India.
- All other chemicals and reagents used in the study were of analytical grade.

9.2.2 Equipments

- Shielded well-type gamma scintillation counter (Caprac-R, Capintec, USA).
- Dose calibrator (Capintec, CRC – 15R, Ramsey N. J., USA)
- Single Photon Emission Computerized Tomography gamma camera (SPECT, LC 75–005, Diacam, Siemens AG, Earlangan, Germany).

- Electronic weighing balance (Mettler AE 163)

9.3 Methods

9.3.1 Radiolabeling of Chitosan and Alginate Microspheres of Carvedilol

The optimized formulations of CRV loaded chitosan (CHCR) and alginate microspheres (ALCR) were labeled with technetium-99m (^{99m}Tc) by direct labeling method as described by Tafaghodi et al (Tafaghodi et al., 2004). The radiolabeling procedure was carried out in the presence of the powerful reducing agent, stannous chloride. The stannous ion reduces 99m-technetium from the +7 oxidation state to the more reactive +4 oxidation state to promote binding. Ten milligrams of microspheres were suspended in the labeling medium containing 0.5 mL of normal saline, 50 µL stannous chloride (5 mg/mL) and 1 mL technetium–99m pertechnetate eluate containing about 3 MCi of activity and pH was adjusted to 6.5 using 0.5 M sodium bicarbonate. The mixture was left under continuous stirring for about 10 min and separated by centrifugation. Microspheres were washed with 2×5ml sterile distilled water and supernatants were collected. The labeled microspheres were washed with acetone (2 × 5 ml). Microspheres were separated by centrifugation and dried by incubation at 60 ^{0}C for 30 min.

9.3.2 Radiolabeling of Lactose

Lactose powder was labeled as above and used in animal studies as a negative control. Lactose powder (20 mg) was dissolved in the above-mentioned labeling media and incubated for 10 min, followed by addition of 10 ml acetone. The labeled lactose was desolvated and precipitated in the presence of acetone. Supernatant was decanted and powder was washed with acetone and dried in 60 ^{0}C for 30 min.

9.3.3 Radiolabeling of Carvedilol

CRV was labeled with technetium-99m (^{99m}Tc) by direct labeling method. Briefly, to 1 mL of drug solution in DMSO and water for injection (2:3) (1 mg/mL), solution containing 40 µL stannous chloride (5 mg/mL) and 0.5 mL technetium–99m pertechnetate eluate containing about 1 MCi of activity was added and pH was

adjusted to 7.0 using 0.5 M sodium bicarbonate. Then the mixture was incubated for 30 min at room temperature.

9.3.4 Determination of Labeling Efficiency of Carvedilol and Its Microspheres

The labeling efficiency was determined by ascending instant thin layer chromatography (ITLC) using silica gel (SG) coated fiber sheets (Gelman Sciences Inc, Ann Arbor, MI). The ITLC was performed using 100% acetone or 0.9% saline as the mobile phase. Around 2 to 3 µL of the radiolabeled complex (in case of microspheres before washing step) was applied at a point 1 cm from the end of an ITLC-SG strip. The strip was developed in acetone or 0.9% saline, and the solvent front was allowed to reach at the top. The strip was cut into two halves, and the radioactivity in each segment was measured in a shielded well-type gamma scintillation counter (Caprac-R, Capintec, USA).

The radiolabeling efficiency was evaluated with ITLC-SG strips as stationary phase and acetone 100% as the mobile phase.

$$\% \text{ Radiolabelling} = \frac{\text{Radioactivity (counts) retained in the lower half of the strip}}{\text{Initial radioactivity associated (total count present) with the strip}} \times 100$$

The effects of stannous chloride concentration, incubation time, and pH on the labeling efficiency were studied by varying the factor in question and keeping the other factors constant.

9.3.5 Stability Study of ^{99m}Tc-CRV/Microsphere Complexes

The in vitro stability study of ^{99m}Tc-CRV/Microsphere Complexes was determined using 0.9% sodium chloride and rabbit serum by ascending thin layer chromatography. The complex (0.1 mL) was mixed with 1.9 mL of normal saline (0.9% sodium chloride) or rabbit serum and incubated at 37°C. ITLC was performed at different time intervals up to 24 hours to assess the stability of the complex.

9.3.6 In Vivo Studies

The in vivo studies were performed following the guidelines approved by the Committee for the Purpose of Control and Supervision of Experiments on Animals (CPCSEA), Ministry of Social Justice and Empowerment, Government of India. The animal protocol was duly approved by the Institutional Animal Ethics Committee.

Twelve normal, healthy, New Zealand white rabbits weighing 2.5 – 3.5 kg were divided in three groups. The animals were fasted overnight prior to the experiment, with free access to water. To first two groups of rabbits, radiolabeled chitosan microspheres (CHCR) and alginate microspheres (ALCR) (approximately 5-7 mg) of carvedilol were administered intranasally using monodose insufflator (Miat, Milano, Italy). To third group, radiolabeled CRV was administered intravenously (0.5 mL) through the dorsal ear vein. At selected time intervals, blood samples were withdrawn from the marginal vein of other ear of the rabbits. The radioactivity in terms of counts per minute (CPM) was measured in a well-type gamma scintillation counter (Caprac-R, Capintec, USA). The animals were conscious during the whole experiment and between each blood sampling they were allowed to move freely within an enclosed area.

9.3.7 Pharmacokinetics Analysis

The noncompartmental pharmacokinetic analysis was performed by Kinetica 5.0 (Thermo Fisher Scientific, USA) and maximum plasma concentration (*C*max), its time of occurrence (*T*max) and the area under the curve (AUC) were determined from the individual time versus radioactivity profiles. The bioavailability (F) of the intranasal (IN) dose of microsphere formulation was calculated with the following equation:

$$F = \frac{AUC_{IN} \times Dose_{IV}}{AUC_{IV} \times Dose_{IN}} \times 100\%$$

Here AUC_{IN} and AUC_{IV} are the individual areas under radioactivity time curves of each rabbit administered microspheres containing CRV ($Dose_{IN}$) intranasally and that of the free CRV solution administered intravenously (IV), respectively.

9.3.8 Gamma Scintigraphy

The deposition, distribution and subsequent clearance of microspheres and lactose were studied by gamma scintigraphy and imaging was performed at 0, 1, 2, 3 and 4 h post administration of microspheres to nasal cavity of rabbits using a Single Photon Emission Computerized Tomography (SPECT, LC 75–005, Diacam, Siemens AG, Earlangan, Germany) gamma camera. The quantification of the data was made defining region of interest (ROI) around the desirable area of the nasal cavity. The highest count rate at 0 min after dosing was assigned a 100% value, which was then used to calculate the percentage remaining for the other time points. In this way the clearance of the formulations from the nasal cavity was evaluated as a decrease in percentage activity against time for each rabbit.

9.3.9 Statistical analysis

Data are presented as mean values ± SD of four determinations. The principal pharmacokinetic measures obtained for the intranasal dose groups were compared statistically using GraphPad™ Instat® Version 3.06 (GraphPad, San Diego, USA). A Student's t-test and one way ANOVA followed by Dunnett's multiple comparison test was performed.

9.4 Results and Discussion

9.4.1 Radiolabeling of Carvedilol and Its Microspheres

In present study we used $^{99m}TcO^{4-}$ because of easy availability, cost effectiveness and low radiation dose. Since half-life of $^{99m}TcO^{4-}$ is 6 h as compared to 60 days for ^{125}I, it presents less radiation burden. ^{99m}Tc has been used to directly label the prepared microspheres based on using stannous chloride as a reducing agent. Chemically, $^{99m}TcO^{4-}$ is a non-reactive species and does not label any compound by direct addition. In ^{99m}Tc-labeling of many compounds, prior reduction of $^{99m}TcO^{4-}$ from 7+ state to a lower oxidation state (4+) is required.

The microspheres (CHCR and ALCR) and CRV were labeled with high efficiency by the direct labeling technique using reduced ^{99m}Tc. Table 9.1 depicts the effect of pH on labeling efficiency. As the pH increased from 6 to 6.5, the radiolabeling efficiency

increased from 93.45% to 98.52% for CHCR and 91.45% to 97.25% for ALCR. Further increase in the pH upto 8 led to reduction in the labeling efficiency. As the pH increased from 6 to 7, the radiolabeling efficiency also increased from 94.37% to 98.84% for CRV. Further increase in the pH upto 8 led to reduction in the labeling efficiency of 90.47%.

Table 9.1 Effect of pH on the % radiolabeling efficiency of Microspheres and Carvedilol

	% Radiolabeled		
pH	**CHCR**	**ALCR**	**CRV**
6	93.45±1.56	91.45±1.94	94.37±1.65
6.5	98.52±1.18	97.25±1.31	96.22±1.15
7	95.22±1.12	94.37±1.68	98.84±1.34
7.5	92.31±1.24	92.64±1.48	93.78±1.38
8	88.36±1.78	90.34±1.32	90.47±1.54

Table 9.2 shows the effect of incubation time on labeling efficiency. The incubation time required for high labeling efficiency was found to be 10 min for CHCR and ALCR; and 30 min for CRV. Further increase in incubation time did not increase the labeling efficiency considerably.

Table 9.2 Effect of Incubation time on the % radiolabeling efficiency of Microspheres and Carvedilol

Incubation time	% Radiolabeled		
(min)	**CHCR**	**ALCR**	**CRV**
0	92.23±1.94	94.68±1.73	95.22±2.48
10	98.25±1.98	97.86±1.84	95.38±1.78
20	98.02±2.14	96.74±2.14	96.34±0.86
30	97.84±1.75	96.12±1.32	98.55±1.94
40	97.55±2.34	95.36±2.36	98.26±1.46

The amount of stannous chloride (reducing agent) used for labeling plays a very decisive role in determining labeling efficiency. A high amount of stannous chloride leads to the formation of radiocolloids (reduced/hydrolyzed $^{99m}TcO^{4-}$), which is undesirable. On the other hand less amount of stannous chloride results in poor labeling (Arulsudar et al., 2003; Thakkar et al., 2004). Table 9.3 shows the effect of various concentrations of stannous chloride ($SnCl_2.2H_2O$) on labeling efficiency. By varying the amount of stannous chloride from 50 to 300 µg, but keeping the other factors like pH and incubation time constant, the influence on labeling efficiency was studied. With increase in stannous chloride amount from 50 to 250 µg, the labeling efficiency was increased from 88.62 % to 98.56% for CHCR and 86.42 % to 97.84% for ALCR. Further increase in the amount of stannous chloride led to a reduction in labeling efficiency. With increase in stannous chloride amount from 50 to 200 µg, the labeling efficiency was increased from 91.45 % to 98.64% for CRV. Further increase in the amount of stannous chloride upto 300 µg led to a reduction in labeling efficiency.

Table 9.3 Effect of Stannous Chloride Concentration on the % radiolabeling efficiency of Microspheres and Carvedilol

Amount of stannous chloride (µg)	% Radiolabeled		
	CHCR	ALCR	CRV
50	88.62±2.12	86.42±1.85	91.45±1.68
100	91.66±1.78	90.56±1.67	95.35±1.25
150	92.24±1.42	93.14±1.24	96.34±0.86
200	96.34±0.84	95.67±0.96	98.64±1.42
250	98.56±1.02	97.84±1.14	88.36±2.16
300	94.38±0.98	92.45±2.15	84.46±1.98

9.4.2 Stability Study of ^{99m}Tc-CRV/Microsphere Complexes

The in vitro stability of the labeled formulations (^{99m}Tc-CRV/Microsphere Complexes) was evaluated in saline and in rabbit serum at 37 ^{0}C for 24 h. All formulations exhibited good in vitro stability as shown in Table 9.4 and 9.5. It is evident from the results that there is insignificant detachment of the radioisotope from the complex. There was no significant reduction in the radiolabeling efficiency upto 24 h which indicates its stability and suitability for in vivo use.

Table 9.4 In Vitro Stability of the ^{99m}Tc-CRV and ^{99m}Tc-Microspheres in Physiological Saline at 37 ^{0}C

	% Radiolabeling efficiency in Saline		
Time (h)	CHCR	ALCR	CRV
0.5	98.12±1.58	97.28±1.24	98.35±1.48
1	97.86±1.64	97.11±1.36	98.22±1.46
2	97.25±2.13	96.86±1.89	97.78±1.21
4	96.38±1.47	96.42±2.19	97.55±1.65
6	96.21±2.12	95.84±1.98	97.34±2.47
24	96.08±1.25	95.56±2.15	96.88±1.22

Table 9.5 In Vitro Stability of the ^{99m}Tc-CRV and ^{99m}Tc-Microspheres in Serum at 37 ^{0}C

	% Radiolabeling efficiency in Serum		
Time (h)	CHCR	ALCR	CRV
0.5	98.04±1.35	97.14±1.31	98.22±1.25
1	97.95±1.22	96.92±1.61	97.88±1.29
2	97.64±1.24	96.35±2.12	97.64±2.74
4	96.92±1.74	96.12±1.54	97.03±1.86
6	96.66±1.98	95.72±2.94	96.67±2.12
24	96.12±1.34	95.32±2.81	96.14±1.36

9.4.3 Pharmacokinetics Studies

The mean blood radioactivity (KCPM/gm) of Carvedilol after intravenous (IV) and of CHCR and ALCR after intranasal administration to rabbits is shown in Table 9.6. The blood kinetics data (blood radioactivity time profiles) of CRV solution injected intravenously and the microsphere formulations (CHCR and ALCR) administered intranasally to rabbits at various time intervals is shown in Figure 9.1.

Table 9.6 Mean blood radioactivity* (KCPM/gm) of Carvedilol after IV and of CHCR and ALCR after Intranasal administration

Time(h)	CRV IV	CHCR Intranasal	ALCR Intranasal
0.25	27.32±2.51	9.29±3.21	4.48±1.22
0.5	22.01±2.53	35.47±2.78	10.15±2.34
1	13.1±1.01	78.79±4.23	29.34±3.24
2	8.67±1.69	53.76±3.89	64.85±4.15
3	7.02±0.89	44.75±2.45	55.36±3.74
4	5.11±1.56	32.93±3.45	45.78±2.57
6	2.88±0.98	25.99±2.98	32.24±2.11
8	1.02±1.02	18.49±1.69	19.46±1.98

* Each value represents the Mean ± SD (n = 4)

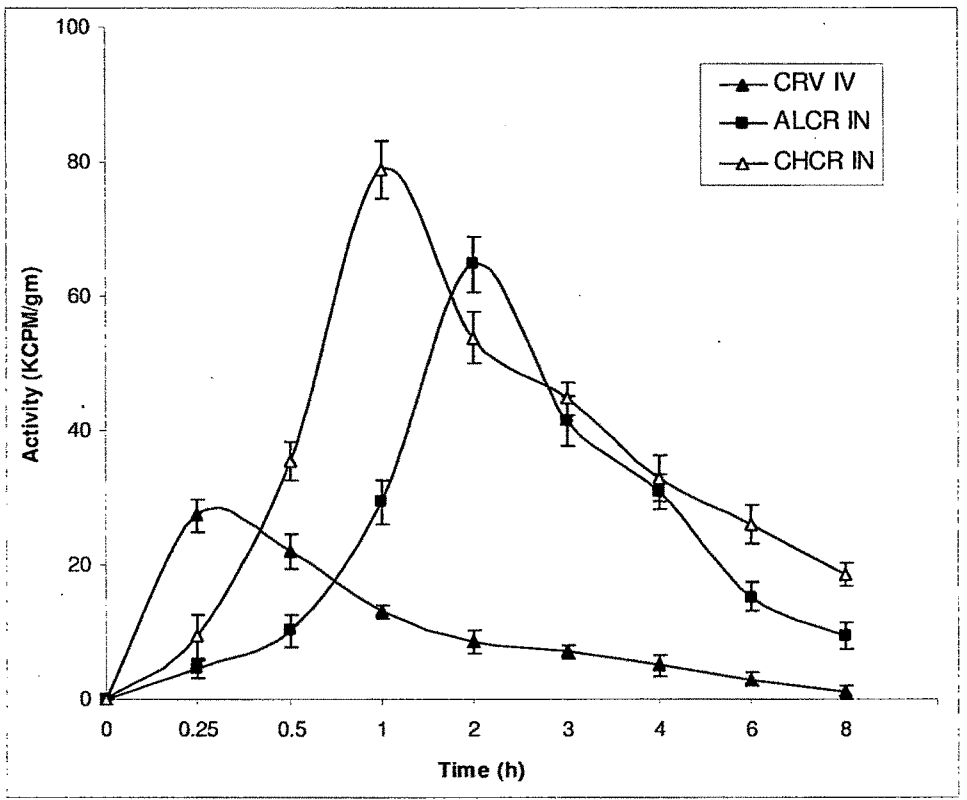

Fig. 9.1 Blood radioactivity time profiles of CRV after administration of microspheres intranasally (IN) (1 mg kg $^{-1}$) and CRV solution intravenously (IV) (0.17 mg kg $^{-1}$) in rabbits.

The relevant pharmacokinetic parameters including maximum concentration (C_{max}), time of maximum plasma concentration (T_{max}), the area under the curve (AUC), half life ($T_{1/2}$), mean residence time (MRT), elimination rate constant (K_{el}) and relative bioavailability (F) are shown in Table 9.7.

Table 9.7 Pharmacokinetic parameters of Carvedilol after IV and of CHCR and ALCR after Intranasal administration in Rabbits

Parameters*	CRV IV	CHCR Intranasal	ALCR Intranasal
C_{max} (KCPM/gm)	-	78.79±4.23	64.85±4.15
T_{max} (h)	-	1.0	2.0
AUC_{0-8h} (KCPM.h/gm)	54.06±6.45	236.59±21.68	215.83±18.56
$AUC_{0-\infty h}$ (KCPM.h/gm)	57.00±7.68	276.23±24.15	247.23±20.48
$T_{1/2}$ (h)	1.99±0.32	2.93±1.24	2.30±0.98
MRT(h)	2.18±0.78	4.31±1.02	4.37±1.31
K_{el} (h^{-1})	0.346±0.092	0.236±0.076	0.300 ±0.084
F (%)	100	74.39	67.87

* Each value represents the Mean ± SD (n = 4)

The C_{max} values observed after intranasal administration of CHCR and ALCR were 78.79±4.23 KCPM/gm and 64.85±4.15 KCPM/gm respectively. The AUC after intranasal administration of CHCR and ALCR were about 236.59±21.68 KCPM.h/gm and 215.83±18.56 KCPM.h/gm respectively which was statistically not significant ($p>0.05$; Student's t test).

T_{max} values were 1.0 and 2.0 h for nasal administration of CHCR and ALCR. The average $T_{1/2}$ values were 2.93±1.24 and 2.30±0.98 h for CHCR and ALCR, respectively, as compared to 1.99±0.32 h following IV administration of CRV.

The MRT was considerably increased following nasal administration of the mucoadhesive formulations of carvedilol (CHCR and ALCR) as compared to IV administration. The average MRT values after nasal administration of CHCR and

ALCR were 4.31±1.02 and 4.37±1.31 h, respectively, as compared to 2.18 ± 0.78 h after IV administration of CRV which were significantly different ($p<0.05$, ANOVA followed by Dunnett's multiple comparison test). Between the two mucoadhesive formulations i. e. CHCR and ALCR, the difference was non significant ($p>0.05$; Student's t test) indicating that there was no formulation variation.

The relative bioavailability (F) for CHCR and ALCR were 74.39% and 67.87% respectively which indicate that nasal administration results in improved absorption of carvedilol from chitosan and alginate microspheres in rabbits. Illum et al. (Illum et al., 2001) described bioadhesive starch microspheres for nasal administration which were retained in the nasal cavity for an extended time period owing to their bioadhesive nature and from which, after gelling, a local high drug concentration was reached. It is reported in previous studies (Gavini E. et al. 2005; Alpar, H.O. et al. 2005) that chitosan has absorption enhancing effect, as it improves the paracellular transport by opening the tight junctions. The high CRV absorption through nasal mucosa may be attributed to the combined effects of bioadhesion and absorption enhancement due to mucoadhesive polymer. It has been demonstrated that the mucoadhesive microparticles have a significant effect on the mucosal uptake of drugs (Pereswetoff-Morath, 1998; Ugwoke et al., 2001). Hence, both the higher local drug concentration and the increased paracellular transport are likely to play an important role in absorption process.

9.4.4 Gamma Scintigraphy

Several methods, both *in vitro* and *in vivo*, have been used to evaluate mucociliary transport rates (Martin et al., 1998; Puchelle et al., 1981; Schipper et al., 1991; Ingels et al., 1991). Advantages of the gamma scintigraphic technique lie in their ability to non-invasively monitor the deposition and clearance of drug formulations, allowing both quantitative and photographic illustrations of distribution and clearance of the radiolabeled formulation. Employing this technique to evaluate the nasal clearance of mucoadhesive preparations requires a radiotracer which is stable and non-diffusible to prevent absorption into the vascular compartment. ^{99m}Tc tracer is reported as technically easy to perform and more representative of ciliary function since it

investigates a large surface of the mucosa as a whole and not the fastest flow rate (Ingels et al., 1995). Therefore, ^{99m}Tc was used in this study.

The nasal clearance characteristics of two microsphere drug delivery systems, CHCR and ALCR, were studied. Lactose powder was used as negative control. The percentage of the formulations cleared from the nasal cavity of rabbits in the time course of study (4 h) is shown in Table 9.8. The clearance data for each formulation from the nasal cavity (ROI) is shown in Fig. 9.2. This data shows that the control lactose powder was cleared rapidly (half-life of nasal clearance was less than 1.0 h), whereas the mucoadhesive delivery systems were retained within the nasal cavity for longer time (half-lives of nasal clearance were >2.5 h). It has been reported that the normal half-life of nasal clearance in man is about 20 min (Schipper et al., 1991). The nasal clearance half-lives of microspheres were higher than normal clearance half-life of human nose (at least four-fold higher), which is representative of high mucoadhesive strength of these particulate systems. Among microsphere formulations (CHCR and ALCR) studied, the lowest clearance rate and highest mucoadhesion was shown by chitosan microspheres (CHCR) followed by alginate microspheres (ALCR). After 4 h, 53.86% of chitosan and 61.55% of alginate microspheres were cleared from nasal cavity while in the same time 87.36% lactose powder was cleared.

Table 9.8 The radioactivity remaining in the rabbit nasal cavity at each time point after administering chitosan microspheres (CHCR), alginate microspheres (ALCR) and lactose powder (control)

Time (h)	Radioactivity (%) in the nasal cavity		
	CHCR	ALCR	Lactose
0	100	100	100
1	71.28	65.25	46.00
2	59.16	52.18	28.32
3	53.42	46.14	21.48
4	46.14	38.45	12.64

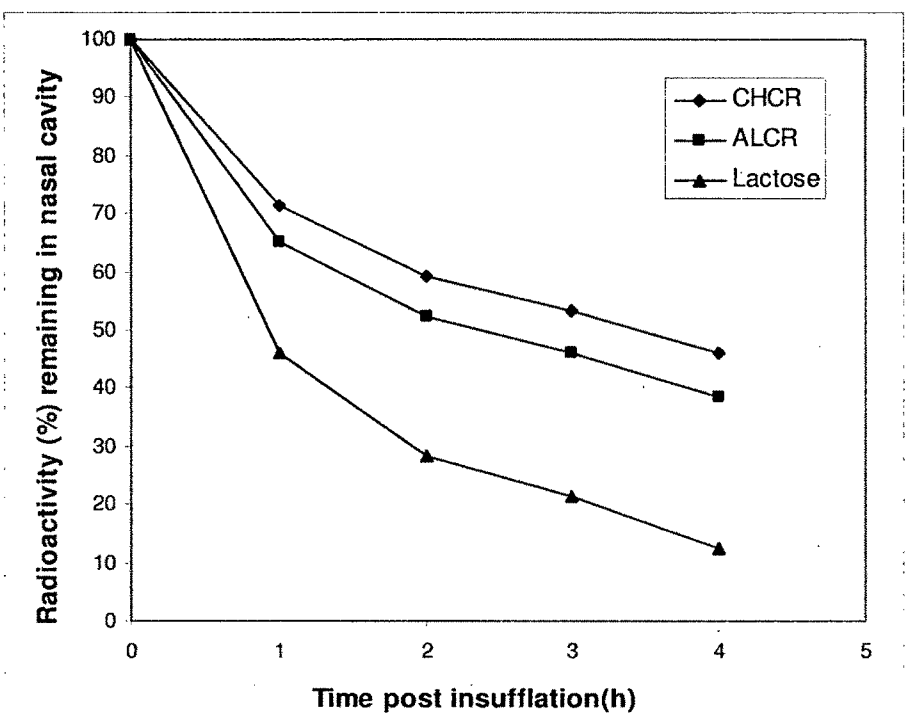

Fig. 9.2 The clearance characteristics of radiolabeled chitosan microspheres (CHCR) and alginate microspheres (ALCR) from the rabbit nasal cavity as compared to lactose powder a control.

In mucoadhesion process, both weak and strong interactions (i.e. van der Waals interaction, hydrogen bonding and ionic bonding) can develop between certain types of functional groups on the polymer (e.g. hydroxyl or carboxyl groups) and the glycoprotein network of the mucus layer or the glycoprotein chains attached to the epithelial cells for example in the nose (Illum et al., 1987). In order for strong adhesive bonds to develop, the establishment of intimate molecular contact between the polymer and glycoprotein chains is essential (Peppas and Buri, 1985). Thus, an important requirement for mucoadhesive polymers is their ability to swell by absorbing water (here from the mucous layer in the nasal cavity) thereby forming a gel-like layer in which environment the interpenetration of polymers and glycoprotein chains can take place and the bindings can form rapidly (Illum et al., 1987).

In administration of microspheric powders, the low clearance of the microsphere systems can be probably attributed to the fact that the microspheres undergo a process of taking up water and swelling, which results in polymer/mucus interaction and increased viscosity of polymer/mucus mixture leading to reduced mucociliary clearance (Illum et al., 1987; Ugwoke et al., 2000).

Studies have shown that polymers with charge density can serve as good mucoadhesive agents (Park and Robinson, 1984; Chickering and Mathiowitz, 1995). Both the microspheres studied in the present work (chitosan and alginate) were ionic and showed good mucoadhesive potential. Compared to lactose powder as control, in nasal cavity, chitosan and alginate microspheres showed a significantly higher mucoadhesion.

The gamma scintigraphy images (Fig. 9.3, Fig. 9.4 and Fig. 9.5) showed that the microsphere powder was spread over a wide area within the nasal cavity of rabbits. The results indicated that the microspheres cleared slowly and were retained for extended periods in the nasal cavity, thereby providing sustained and enhanced drug absorption from the nasal mucosa, as confirmed from pharmacokinetic studies.

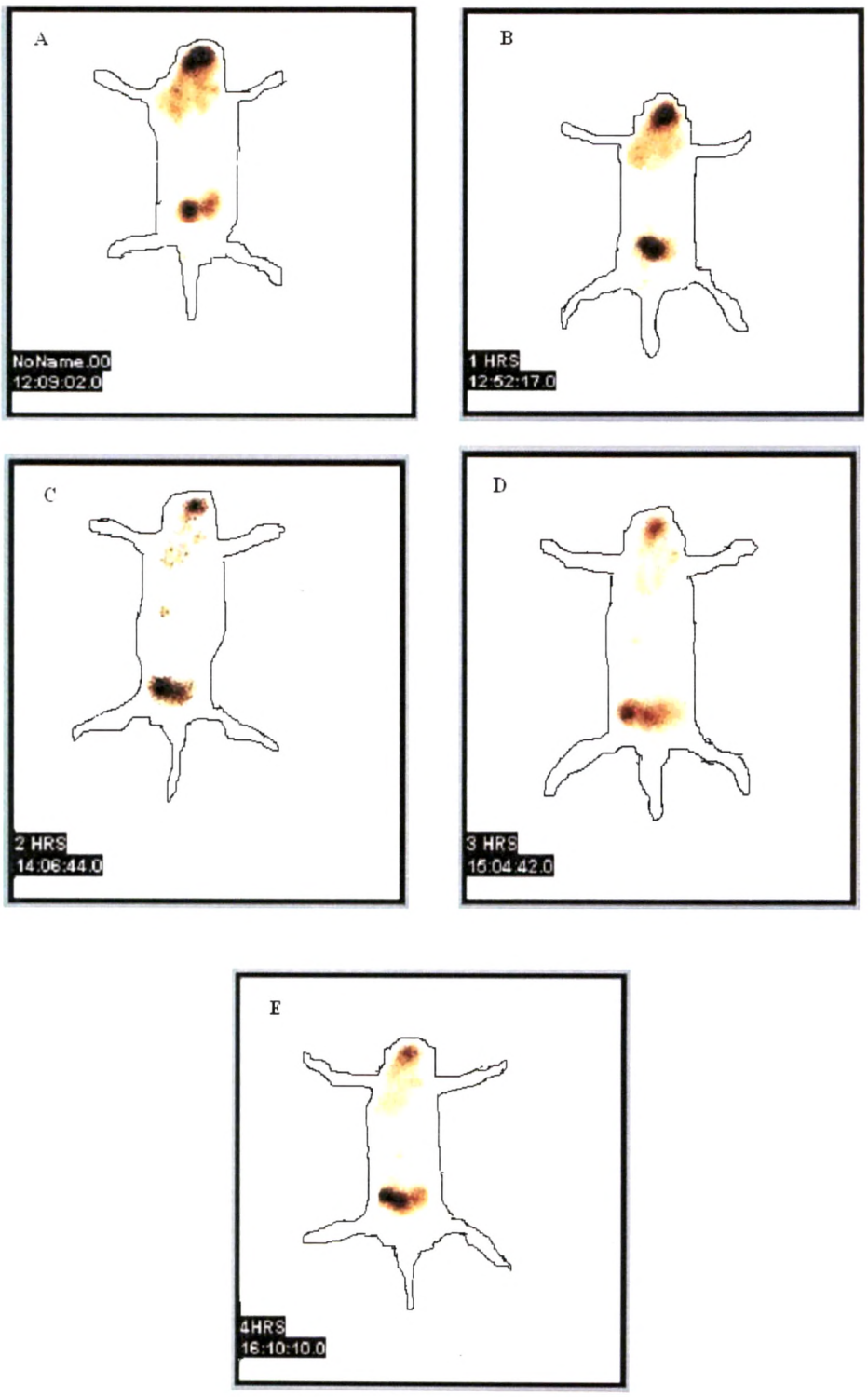

Fig. 9.3 Scintigraphic rabbit whole body images showing radioactivity in the nasal cavity after administration of ^{99m}Tc labeled chitosan microspheres of carvedilol (CHCR) at different times of 0 h (A), 1 h (B), 2 h (C), 3 h (D) and 4 h (E) post insufflation.

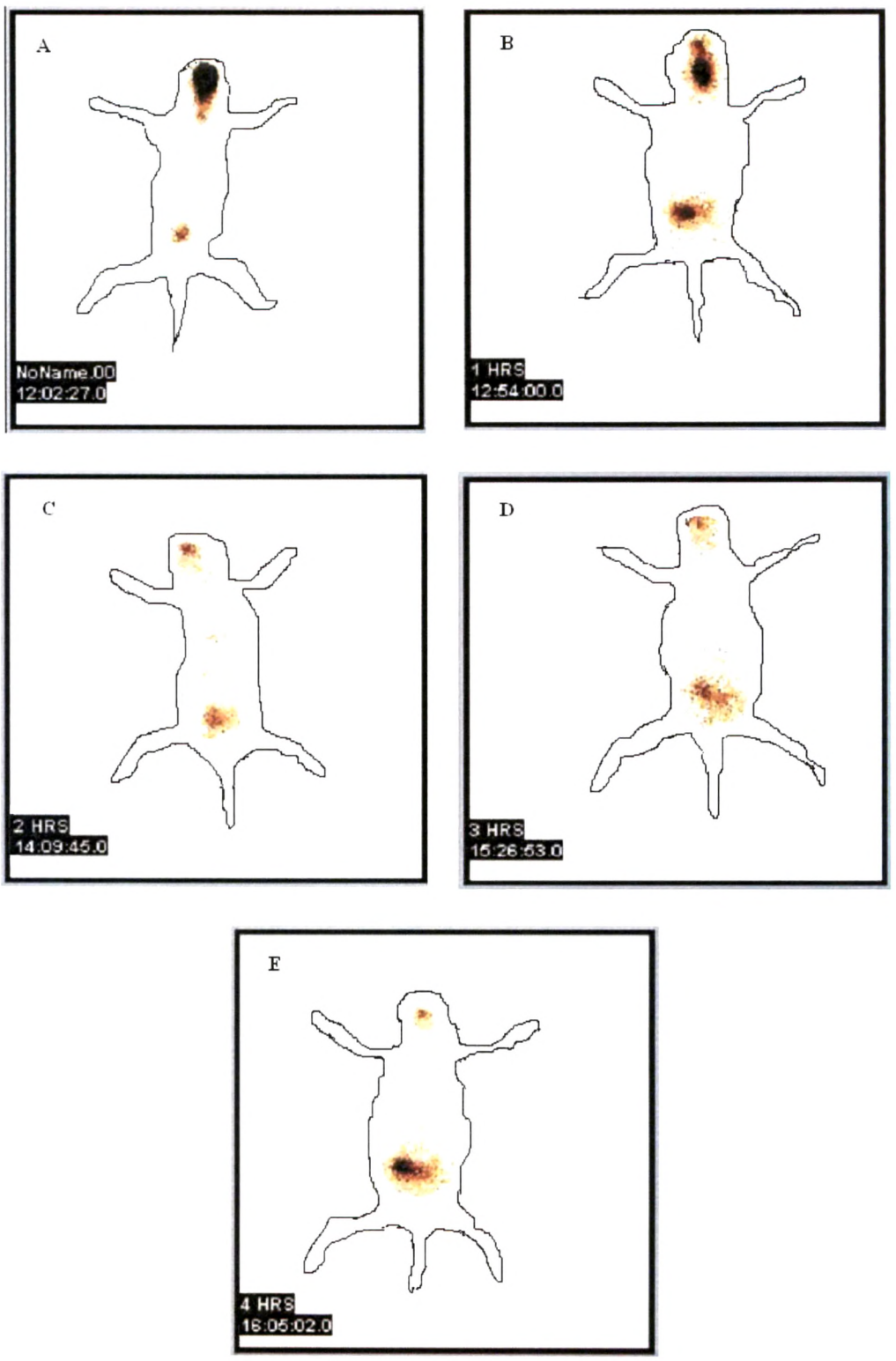

Fig. 9.4 Scintigraphic rabbit whole body images showing radioactivity in the nasal cavity after administration of ^{99m}Tc labeled alginate microspheres of carvedilol (ALCR) at different times of 0 h (A), 1 h (B), 2 h (C), 3 h (D) and 4 h (E) post insufflation.

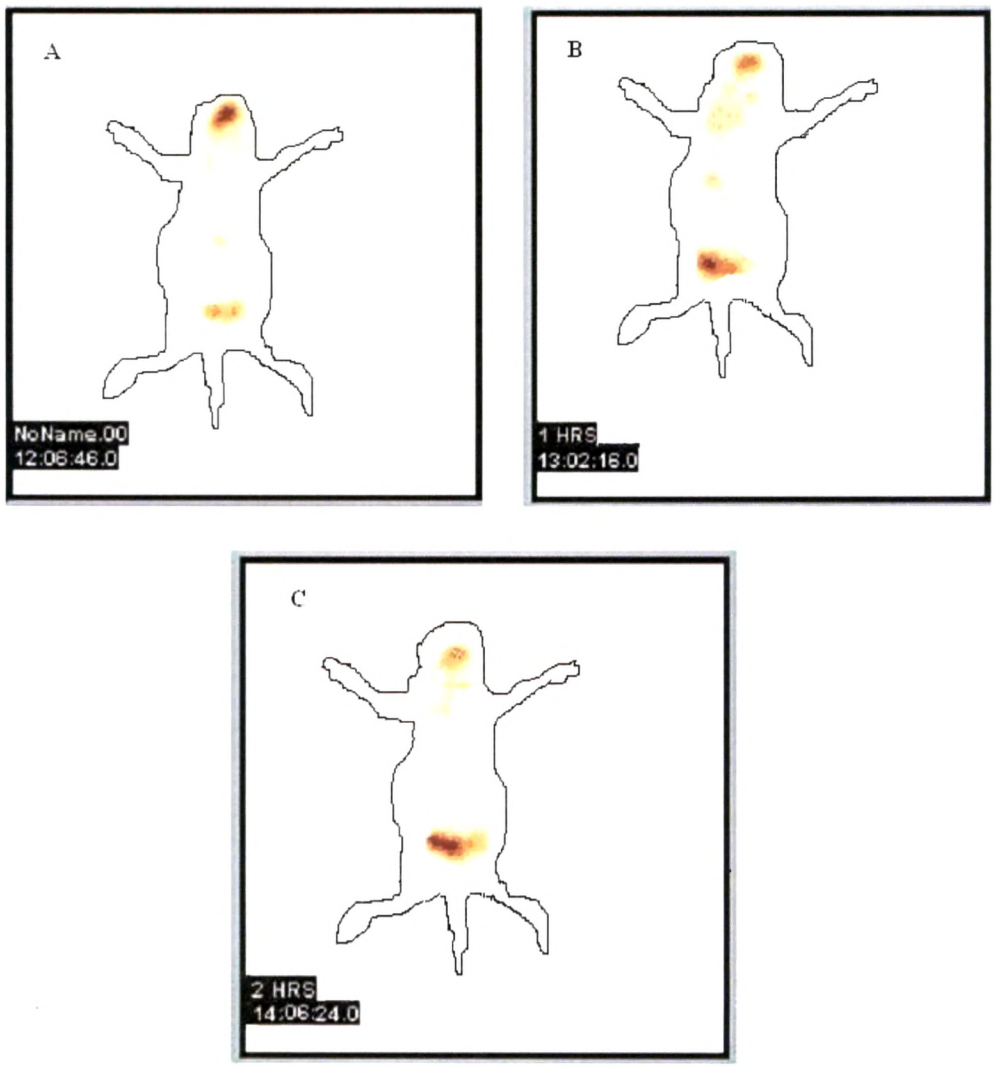

Fig. 9.5 Scintigraphic rabbit whole body images showing radioactivity in the nasal cavity after administration of ^{99m}Tc labeled lactose powder (control) at different times of 0 h (A), 1 h (B) and 2 h (C) post insufflation.

REFERENCES

Alpar, H. O.; Somavarapu, S.; Atuah, K. N.; Bramwell, V. W. Biodegradable mucoadhesive particulates for nasal and pulmonary antigen and DNA delivery. *Adv. Drug Deliv. Rev.* **2005,** 57, 411–430.

Chickering, D.; Mathiowitz, F. Bioadhesive microspheres: I. A novel electrobalance-based method to study adhesive interactions between individual microspheres and intestinal mucosa. *J. Controlled Release* **1995**, 34, 251–261.

Digenis, G. A.; Sandefer, E. P.; Page, R. C.; Doll, W. J. Gamma scintigraphy: an evolving technology in pharmaceutical formulation development – Part 1. Pharm. Sci. Tech. Today, 1998, 1(3), 100 – 107.

Gavini, E.; Rassu, G.; Sanna, V.; Cossu, M.; Giunchedi, P. Mucoadhesive microspheres for nasal administration of an antiemetic drug, metoclopramide: in-vitro/ex-vivo studies. *J. Pharm. Pharmacol.* **2005,** 57, 287-294.

Illum, L.; Jorgensen, H.; Bisgaard, H.; Krogsgaard, O.; Rossing, N. Bioadhesive microspheres as a potential nasal drug delivery system. *Int. J. Pharm.* **1987**, 39, 189–199.

Illum, L.; Fisher, A. N.; Jabbal-Gill, I.; Davis, S. S. Bioadhesive starch microspheres and absorption enhancing agents act synergistically to enhance the nasal absorption of polypeptides. *Int. J. Pharm.* **2001,** 222, 109–119.

Ingels, K, Van Hoom, V.; Obrie, E.; Osmanagaoglu, K. A modified technetium-99m isotope test to measure nasal mucocillary transport: comparison with the saccharine-dye test. *Eur. Arch. Otorhinolaryngol.* **1995**, 252, 340–343.

Marttin, E.; Schipper, N. G. M.; Verhoef, J. C.; Merkus, F. W. H. M. Nasal mucociliary clearance as a factor in nasal drug delivery. *Adv. Drug Deliv. Rev.* **1998**, 29, 13–38.

Park, K., Robinson, J. R. Bioadhesive polymers as platforms for oral-controlled drug delivery: method to study bioadhesion. *Int. J. Pharm.* **1984**, 19, 107–127.

Peppas, N. A.; Buri, P. A. Surface, interfacial and molecular aspects of polymer bioadhesion on soft tissues. *J. Controlled Release* **1985**, 2, 257–275.

Pereswetoff-Morath, L. Microspheres as nasal drug delivery systems. *Adv. Drug Deliv. Rev.* **1998,** 29, 185-194.

Puchelle, E.; Aug, F.; Pham, Q. T.; Bertrand, A. Comparison of three methods for measuring nasal mucociliary clearance in man. *Acta Otolaryngol.* **1981**, 91, 297–303.

Saha G. B. Fundamentals of Nuclear Pharmacy, 5th Edition, Springer, New York, 2004, 79-109

Schipper, N. G. M.; Verhoef, J. C.; Merkus, F. W. H. M. The nasal mucociliary clearance: relevance to nasal drug delivery. *Pharm. Res.* **1991**, 8, 807–814.

Tafaghodi, M.; Tabassi, S. A. S.; Jaafari, M. R.; Zakavi, S. R.; Momen-nejad, M. Evaluation of the clearance characteristics of various microspheres in the human nose by gamma-scintigraphy. *Int. J. Pharm.* **2004,** 280, 125–135.

Ugwoke, M. I.; Agu, R. U.; Vanbilloen, H.; Baetens, J.; Augustijns, P.; Verbeke, N.; Mortelmans, L.; Verbruggen, A.; Kinget, R.; Bormans, G. Scintigraphic evaluation in rabbits of nasal drug delivery systems based on Carbopol 971p® and carboxymethylcellulose. *J. Controlled Release* **2000**, 68, 207–214.

Ugwoke, M. I.; Verbeke, N.; Kinget, R. The biopharmaceutical aspects of nasal mucoadhesive drug delivery. *J. Pharm. Pharmacol.* **2001,** 53, 3–22.